

# A Novel View on the Inner Crusts of Neo-Neutron Stars: exotic light nuclei, diffusional and thermodynamical stability

Mikhail V. Beznogov<sup>1,\*</sup> and Adriana R. Raduta<sup>1,†</sup>

<sup>1</sup>*National Institute for Physics and Nuclear Engineering (IFIN-HH), RO-077125 Bucharest, Romania*

(Dated: April 18, 2025)

Based on an extended nuclear statistical equilibrium model, we investigate the properties of non-accreted crusts of young and warm neo-neutron stars, i.e., of finite-temperature inhomogeneous dense matter in beta equilibrium. We present two novel results and one known, but frequently ignored property of such matter. The first new feature is the appearance, in the deep inner crust, of an extensive and almost pure  $^{14}\text{He}$  layer that extends up to the density of the transition to homogeneous matter. This layer may challenge the idea of nuclear pasta phases, significantly impact the transport properties and the crust crystallization process. Second, we raise the question of the (in)stability of the inner crust with respect to diffusion of ions (buoyancy) and demonstrate that our crust is stable, in contrast with the predictions of some other models. Finally, we show that subsaturated stellar matter is thermodynamically stable with respect to density fluctuations, which rules out a first-order phase transition between inhomogeneous and homogeneous phases.

## I. INTRODUCTION

An important stage of the evolution of neutron stars (NSs) is the neo-NS phase [1]. It begins at the end of the proto-NS phase, when the star's temperature drops below  $\approx 2$  MeV, and its material becomes transparent to neutrinos, and lasts for about a day. While NS cores acquire their final composition and size during the proto-NS phase, NS crusts form and crystallize [1–3] during the neo-NS stage. The crust crystallization epoch roughly coincides with the time when the nuclear statistical equilibrium (NSE) freezes, meaning that subsequent modifications of the crust composition can only occur through a limited subset of nuclear reactions and at a slow pace [4, 5]. Consequently, in reality an NS crust might never reach the “cold catalyzed” state, which is usually considered a standard paradigm for mature isolated NSs [4, 6]. For accreting NSs the initial composition of the crust is also important, especially in the case of partial accretion [7]. Thus, since the crust formation process sets the initial composition, it is necessary to investigate it in more details. Such an investigation requires dedicated simulations that combine thermal evolution with evolution of chemical composition and mechanical structure. To our knowledge, no such studies are available so far.

Some steps in this direction were taken in Ref. [1]. As a further step, in this Letter we consider the nuclear composition of warm inhomogeneous matter with densities lower than the nuclear saturation density ( $n_{\text{sat}} \approx 0.16 \text{ fm}^{-3} \approx 2 \cdot 10^{14} \text{ g/cm}^3$ ) and in beta equilibrium. We also discuss the questions of the thermodynamic stability of NS crusts with respect to density fluctuation and the stability with respect to diffusion of ions (buoyancy). The presented results were obtained employing an extended NSE model [8] and a high-performance code that we developed specifically for this purpose. In addition, the composition of the cold NS crusts was calculated as a low-temperature limit of the finite-temperature results.

## II. FORMALISM

For densities lower than  $n_{\text{sat}}$  and temperatures lower than a dozen MeV, stellar matter consists of a mixture of nuclei (clusters, ions), nucleons, leptons, and photons. Charged leptons are essential for compensating for the positive charge of the protons. Assuming that charge neutrality holds locally, one gets  $n_p = n_e + n_\mu$ , where  $n_{e/\mu}$  stands for the (net) number density of electrons/muons. The only significant interaction between electrons and protons is the electrostatic one. The electrons and photons interact weakly and are treated as ideal Fermi and Bose gases, respectively. Neutrinos are not necessarily in equilibrium with the rest of matter and are disregarded here.

Below we briefly describe our extended NSE model. The complete derivation will be published elsewhere [8]. Similar derivation can also be found in Ref. [9]. In NSE, which is expected to hold for temperatures  $T \gtrsim 0.3 - 0.4$  MeV [10], the only intrinsic properties of the  $(A, Z)$ -nuclei (with  $A$  being the mass number and  $Z$  being the charge number) that enter the abundance of those nuclei are the internal partition function  $z_{A,Z}^{\text{int}}$  and the binding energy  $B_{A,Z}$ . In our model, nuclei with  $A \geq 2$  are supposed to form an ideal gas, while unbound nucleons are treated within the mean-field theory of nuclear matter (NM). Interactions between nuclei and unbound nucleons are phenomenologically implemented via the excluded volume approximation, which proves essential for an adequate description of densities in the proximity of  $n_{\text{sat}}$ . Coulomb interactions between protons and electrons and among the electrons are accounted for within the Wigner-Seitz approximation [11], as customarily in the literature. Our pool of nuclei consists of nuclides present in the experimental mass table AME 2020 [12] and nuclides for which the nuclear masses have been evaluated with the 10 parameter model by Duflo and Zuker [13]; experimental values are preferred for nuclides for which both tables provide data. The internal partition functions,  $z_{A,Z}^{\text{int}} = g_{\text{G.S.}} + \int_0^{B(A,Z)} d\epsilon \exp(-\epsilon/T) \rho(\epsilon)$ , account for the spin degeneracy of the ground state and the thermal excitations of high energy levels. The second contribution is estimated using the back-shifted Fermi gas level density from Refs. [14, 15]. The results presented here correspond to the non-relativistic

\* mikhail.beznogov@nipne.ro

† araduta@nipne.ro

model of NM [16, 17] but all important features would persist should this formalism be replaced with the covariant density functional theory of dense matter. In particular, the BSk25 [18] version of the Brussels extended Skyrme effective nucleon-nucleon interaction was used.

The key feature of NSE is that the chemical equilibrium with respect to electrostatic and strong interactions is assumed to be achieved. This allows one to express the chemical potential of an  $(A, Z)$ -nucleus in terms of the chemical potentials of unbound neutrons and protons,

$$\mu_{A,Z} = (A - Z)\mu_n + Z\mu_p. \quad (2.1)$$

From chemical equilibrium one can further derive the expression for the number of  $(A, Z)$ -nuclei in a given volume, which, combined with the equations of mass and charge conservation, fully determines the state of matter for a fixed total baryon density  $n_B$ , proton fraction  $Y_p$ , and temperature  $T$ .

To take into account the saturation density dependence on the isospin asymmetry, we wrote the intrinsic volume of one  $(A, Z)$ -cluster as  $v_{A,Z} = A/n_{\text{sat}}(\delta)$  with  $\delta = 1 - 2Z/A$ . This seemingly small correction has a noticeable impact on the composition and energetics of matter as well as on the density of the transition to homogeneous matter. The transition itself has to be discussed in more details here. In our calculations we observed three mechanisms of the transition: 1) the homogeneous matter becomes energetically favorable; 2) the clusters occupy the whole volume; 3) the gas of unbound nucleons occupy the whole volume. Only in the last case the transition was smooth and occurred “naturally”. In two other cases switching to homogeneous matter produced discontinuities in thermodynamic functions because excluded volume coupling and Coulomb interaction generate shifts in chemical potentials that disappear in homogeneous matter. Thus, we had to design a special matching procedure, based on pressure, in order to facilitate a smooth transition in *all* cases and avoid discontinuities. We insist, however, that it is not a Maxwell construction. First, because, as we show in the next section, unlike the commonly held point of view, this transition is *not* a first-order phase transition if electrons are accounted for. Second, because Maxwell constructions require the values of all intensive state variables to be equal in the coexisting phases, which cannot be realized here.

The beta equilibrium configurations were computed within zero-temperature approximation by requiring that  $\mu_p = \mu_n + \mu_e$ , which corresponds to vanishing lepton chemical potential. However, as discussed in Ref. [19] at  $T \gtrsim 1$  MeV beta equilibrium cannot be obtained from a simple zero-temperature relation even if neutrinos are still in the free-streaming regime. Thus, we had to consider the lower end of the neo-NS temperature range in our investigations. In particular, the results presented in the next section correspond to  $T = 0.4$  MeV. We also present some results in the limit of  $T = 0.1$  MeV to compare them with some of the existing zero-temperature equations of state (EOSs) of the crust.

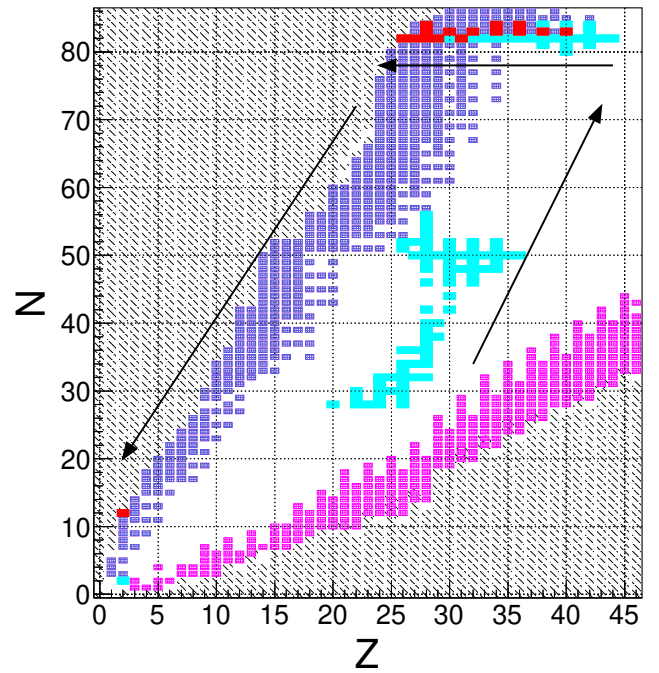


Figure 1. Composition of neo-NS crust and visualization of the employed mass tables. White areas represent the nuclides with positive neutron and proton separation energies, while the nuclides with negative neutron and proton separation energies are marked in violet and magenta, respectively. The gray hatched domain corresponds to nuclei for which nuclear mass data are not available. Cyan and red show the “stable” and beyond neutron-drip nuclei present in the crust. The arrows show the direction of increase of  $n_B$ .  $T = 0.4$  MeV. BSk25 [18] effective interaction is used here.

### III. RESULTS & DISCUSSION

Let us start with the composition of the crust. The most interesting and novel result here is the rapid change of composition from heavy nuclei with  $A \sim 100$  to an almost pure layer of  $^{14}\text{He}$  in the innermost shells of neo-NS crusts, see Figs. 1 and 2. This layer persists over the whole temperature domain, including  $T = 0.1$  MeV, which is beyond the validity limit of the NSE.  $^{14}\text{He}$  stems from the DZ10 table [13]; it has a binding energy of 19.3 MeV and a negative neutron separation energy,  $S_n = -1.29$  MeV.

Figure 1 provides an overview of the species present in the crust for BSk25 [18] effective interaction and  $T = 0.4$  MeV. Nuclides with positive neutron and proton separation energies are marked in cyan; nuclides beyond neutron-drip are marked in red. The arrows provide a general idea of the direction of the increase in density. The preference for nuclides with magic number of neutrons (especially 50 and 82) is clearly visible. Some features of the employed nuclear mass tables are displayed as well, see the figure caption. Note that the mass tables extend up to  $A = 297$ , but the ranges of the axes were reduced for better visibility.

Further insight into crust composition is provided in Fig. 2, which illustrates the dependence of the mass fractions of “heavy” ( $A \geq 20$ ) nuclei,  $^{14}\text{He}$  and unbound nucleons (bot-

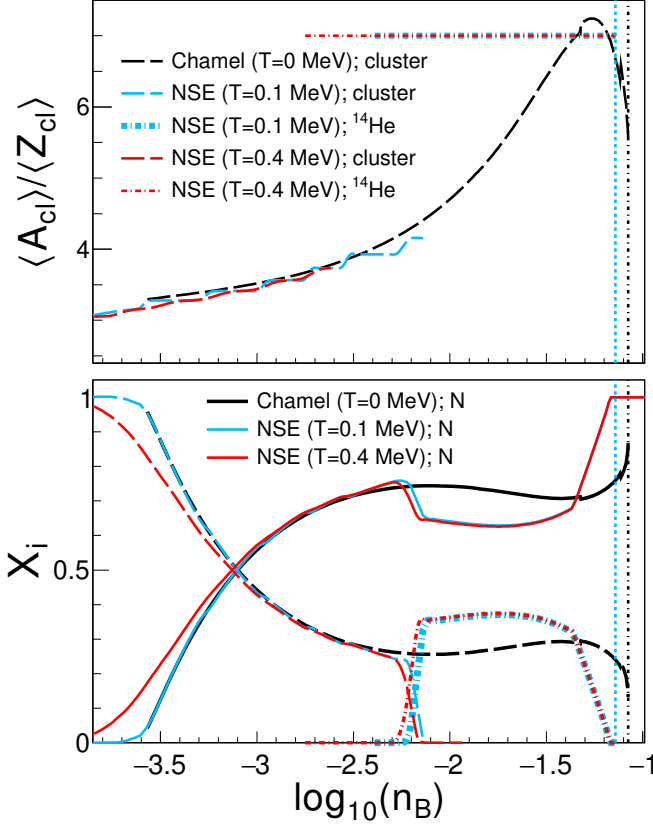


Figure 2. Mass fractions of “heavy” ( $A \geq 20$ ) nuclei,  $^{14}\text{He}$  and unbound nucleons (bottom panel) and mass to charge numbers ratio (top panel) as functions of baryon number density. NSE results obtained in this work for beta-equilibrated matter are compared with the zero temperature results of Ref. [20]. In both cases BSk25 [18] effective interaction was employed. Vertical dotted lines mark the transition to homogeneous matter,  $n_{tr} = 0.0742 \text{ fm}^{-3}$  and  $0.0839 \text{ fm}^{-3}$  for NSE results and the results of Ref. [20], respectively.

tom panel) and the  $A_{cl}/Z_{cl}$  ratio (top panel) on the total baryon density  $n_B$  for  $T = 0.4 \text{ MeV}$  (red curves) and  $T = 0.1 \text{ MeV}$  (blue curves). The predictions of the extended Thomas Fermi plus Strutinsky integral model of Ref. [20] is demonstrated as well for comparison (black curves). All results correspond to BSk25 [18] effective interaction. The transition density to homogeneous matter for our NSE model at the lowest temperature and the model of Ref. [20] are indicated with vertical dotted lines. Figure 2 shows that for  $n_B \lesssim 0.006 \text{ fm}^{-3}$  and  $T = 0.1 \text{ MeV}$  NSE provides the same mass fractions as the model of Ref. [20]; for other effective interactions (not shown) the agreement is also very good. This indicates that the mass sharing is mainly determined by the effective interaction and also justifies the NSE results obtained for temperatures beyond the validity limits. Quite remarkably, the  $A_{cl}/Z_{cl}$  ratios are also very similar, even though the values of  $A_{cl}$  and  $Z_{cl}$  predicted by NSE are very different from those of Ref. [20], which allows for much more massive and much more neutron-rich clusters.

From Fig. 2 one can see that the  $^{14}\text{He}$  layer rapidly becomes abundant at  $n_B \approx 0.006 \text{ fm}^{-3}$  and extends up to the transition

density. It comprises almost 40% of the mass and is responsible for the depletion of the gas of unbound nucleons, as well as a sudden increase of the  $A_{cl}/Z_{cl}$  ratio to 7. Note that the onset density and the mass fraction depend on the effective interaction with BSk25 providing the lowest onset density and the highest mass fraction among all the interactions that we have tested. The emergence of the  $^{14}\text{He}$  layer causes our results to depart from the results of Ref. [20].

The “steps” caused by the shell and odd-even effects coming from the employed experimental and evaluated mass tables are very clearly seen in the top panel at  $T = 0.1 \text{ MeV}$  (blue dashed curve). One can also see how these “steps” are smoothed out, but not completely, by temperature (red dashed curve). Other effects of temperature can be assessed by comparing the blue and red curves in the bottom panel. There are some quantitative differences in the mass fractions for  $n_B \lesssim 10^{-3} \text{ fm}^{-3}$ , but they become negligible at higher densities.  $^{14}\text{He}$  appears at somewhat lower density for a higher temperature, but the domain where it is dominant is almost the same for both considered temperatures.

Replacement of more massive nuclei by  $^{14}\text{He}$  in the deepest parts of the inner crust is unexpected and, to the best of our knowledge, has never been discussed before. We explain this situation by the inability of Hartree-Fock, extended Thomas Fermi, or phenomenological liquid drop models to deal with light nuclides that have essentially no “bulk”. The failure of other (extended) NSE models to account for this exotic light cluster can be attributed either to its omission from the pool of nuclei or convergence issues at densities of about a fraction of  $n_{\text{sat}}$ . If confirmed,  $^{14}\text{He}$  would significantly change our view of the inner crust and challenge many works devoted to the “nuclear pasta” phase.

First, the high purity of the  $^{14}\text{He}$  layer may lead to very different thermal and electrical conductivities compared to the layers made of massive nuclei. Indeed, in our case the impurity parameter [5, 21]  $Q_{\text{imp}}$  is almost density independent and is  $\lesssim 0.01$  in the whole region where  $^{14}\text{He}$  is dominant and  $T < 0.5 \text{ MeV}$ . In contrast, in Ref. [5] the impurity parameter oscillates a lot as a function of  $n_B$  in the range  $0.01 \lesssim Q_{\text{imp}} \lesssim 100$  for  $0.01 \leq n_B \leq 0.08 \text{ fm}^{-3}$  and  $T \approx 0.27 \text{ MeV}$  with the amplitude and position of the extrema depending on the effective interaction. This feature will affect the interpretation of crustal cooling in low-mass X-ray binaries [22] (see, e.g., Refs. [5, 7, 23]) as well as magneto-rotational evolution of NSs (see, e.g., Ref. [24]).

Second,  $^{14}\text{He}$  will alter the process of crust crystallization, which is essential for crust structure, composition, and transport properties. We remind that the crust crystallizes as a Coulomb crystal and, in the simplest one-component plasma approximation, the crystallization temperature is proportional to  $Z^2$  [4]. Thus, a sudden change of  $Z$  from  $20 \leq Z \leq 40$  to  $Z = 2$  will diminish the crystallization temperature by a factor of 100 to 400. Moreover,  $^{14}\text{He}$  leads to a configuration where more dilute shallower layers of the crust might already be frozen, while the deeper and denser layers still remain liquid. Also important is the ion plasma temperature, which delineates the classical and quantum plasma regimes and is proportional to  $Z$  [21]. Again, the onset of  $^{14}\text{He}$  will cause a sudden change

in this temperature.

Since we employed experimental and evaluated mass tables, all our results assume implicitly that in dense media all nuclei, including  $^{14}\text{He}$ , have the same properties as in vacuum. Although this is certainly not true, the studies available to date [25, 26] are not sufficient for a realistic treatment of the nuclear binding energies over the whole mass table and for arbitrary densities and isospin compositions of the medium. In defense of our results, we only remind that all nuclei predicted to exist in the inner crust are beyond the neutron drip (by its very definition). Of course, further investigation of this issue is necessary, possibly accounting for other exotic light clusters that may be relevant for the crust, e.g., tetra-neutron resonances [27, 28].

The next aspect that we want to discuss in this Letter is the problem of buoyancy and the (in)stability of the inner crust with respect to diffusion of ions. For an electrically neutral multicomponent plasma in an external gravitational field, the velocity of gravitational separation (sedimentation) of the ions is determined by the “effective weight”  $A/Z$  (see, e.g., Refs. [29, 30]). To simplify the explanation, let us name the ions at higher  $n_B$  as ions type 2 and the ions at lower  $n_B$  as type 1. Type 2 ions are located deeper, below type 1 ions, as the density in the crust increases with depth (counting from the surface of an NS). As long as the  $A/Z$  ratio is a non-decreasing function of  $n_B$ , the configuration is stable, type 2 ions tend to diffuse downward or stay where they are if already in diffusive equilibrium. Likewise, type 1 ions tend to diffuse upward or stay where they are. However, if the “effective weight” decreases with  $n_B$ , the situation becomes unstable: type 2 ions will tend to diffuse upward and type 1 ions downward. This is similar to the classical Rayleigh–Taylor instability, only here the buoyancy is determined by the  $A/Z$  ratio. If type 2 and type 1 ions interchange with each other to satisfy the diffusion equilibrium, they will move out of chemical equilibrium (2.1). Hence, such a situation is unstable.

This buoyancy issue is complicated as diffusion and cooling timescales can be comparable. We do not have an estimate of the diffusion timescale for the conditions (temperatures and densities) of the inner crust, but for the outer crust, the gravitational separation of ions occurs on a timescale of one day [31]. When the crust crystallizes, the diffusion becomes strongly suppressed, and this instability becomes much less relevant. Thus, the whole buoyancy problem is important for the neo-NS evolutionary phase. As discussed above regarding  $^{14}\text{He}$ , the crystallization temperature depends strongly on the composition, but to estimate the cooling timescale we can employ the NSE freezing out temperature ( $T \approx 0.3 - 0.4$  MeV [10]) as a proxy. For  $T \approx 0.4$  MeV, this timescale is roughly one day [1][32]. Since the diffusion and cooling timescales seem to be comparable, a cooling simulation that takes into account diffusion in the inner crust is necessary in order to further investigate the question of buoyancy in the inner crust, but this is way beyond the scope of this Letter. Note that the above estimates are relevant for isolated (non-accreting) NSs.

As can be seen from the top panel of Fig. 2, our NSE model is stable with respect to diffusion, and  $^{14}\text{He}$  plays a big role in this aspect. The model of Ref. [20], however, is not stable

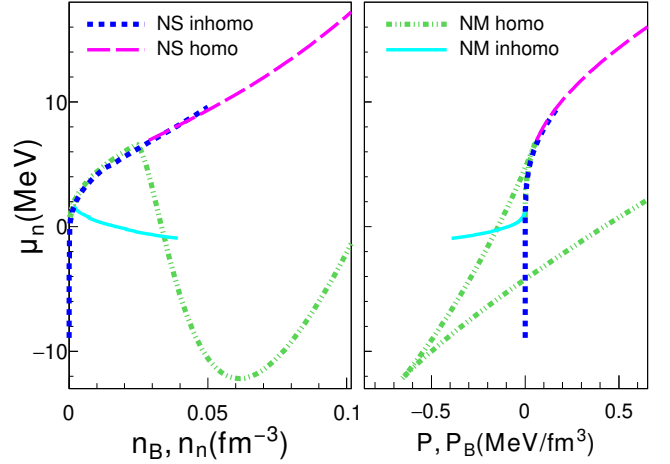


Figure 3. Thermodynamic (in)stability of cold NS matter ( $T = 0.1$  MeV). Left and right panels show the baryon chemical potential ( $\mu_B = \mu_n$ ) as a function of particle number density ( $n_B$  or  $n_n$ ) and pressure ( $P$  or  $P_B$ ), respectively. NM without Coulomb interaction is computed at a fixed  $\mu_p = -30$  MeV. NS matter with electrons is computed at a fixed  $\mu_{lep} = 0$  (beta equilibrium). The effective interaction is BBSk1 [8]. See text for details.

with respect to diffusion as it has a range of densities where the  $A_{cl}/Z_{cl}$  ratio decreases. We have also checked some other existing crustal EOSs. All EOSs of Ref. [20] as well as GPPVA EOSs [33] are unstable. On the other hand, NV EOS [34], D1M and D1M\* EOSs [35], and SPG EOSs [36] are stable.

The issue of the (in)stability of the inner crust with respect to diffusion was raised in Refs. [37, 38] in the context of accreted crusts and diffusion of unbound neutrons. We have demonstrated here that the ion subsystem may also suffer from diffusional instabilities regardless of the unbound neutrons. In addition, our findings are applicable to non-accreted crusts. Notice furthermore that there are other components entering the diffusive flux that might compensate for the gravitational separation term. However, they are proportional to the gradients of densities and, therefore, cannot be “adjusted” freely without violating the overall hydrostatic equilibrium (see a discussion in Ref. [37]).

The last question that we want to discuss in this Letter is the question of thermodynamic stability of NS matter. Since the domain of density-driven instabilities in dilute homogeneous NM shrinks with increasing temperature [39–42], it is sufficient to analyze the case of the lowest considered temperature,  $T = 0.1$  MeV.

To investigate the question of thermodynamic stability of a multicomponent system, one may plot, for example, the chemical potential of one component as a function of its conjugate number density while keeping the chemical potential of the other component fixed [40, 43]. If there is a range of densities where the chemical potential decreases with increasing density, then the system has an instability with respect to phase separation. In Fig. 3 we compare four systems: inhomogeneous (cyan) and homogeneous (green) NM without Coulomb interaction [44] and inhomogeneous (blue) and homogeneous



(magenta) NS matter (i.e., with electrons and in beta equilibrium). For NM we plot  $\mu_n$  as a function of  $n_n$  (left panel) at a fixed  $\mu_p = -30$  MeV; rest-mass contributions are subtracted. For NS matter, we plot the baryon chemical potential  $\mu_B (= \mu_n)$  as a function of  $n_B$  (left panel) for a fixed lepton chemical potential  $\mu_{lep} = 0$  (beta equilibrium). From the left panel one can immediately see that both inhomogeneous and homogeneous NM have regions where  $\mu_n$  decreases with  $n_n$  and, thus, both are thermodynamically unstable with respect to the first-order phase transition. However, for both inhomogeneous and homogeneous NS matter  $\mu_B$  is a monotonically increasing function of  $n_B$ . Such matter is thermodynamically stable; there is no *first-order* phase transition between inhomogeneous and homogeneous NS matter. The right panel provides further information in terms of  $\mu_n$  vs  $P_B$  (baryonic pressure) plot for NM at fixed  $\mu_p = -30$  MeV and  $\mu_B (= \mu_n)$  vs  $P$  (total pressure) for NS matter at fixed  $\mu_{lep} = 0$ . Over the phase instability domains, the  $\mu_n(P_B)$  curves (green and cyan) are concave. Whenever the system is stable, these curves are convex.

This conclusion is not exactly new. The thermodynamic instability of inhomogeneous [25, 45, 46] and homogeneous [39–42] NM is well studied in the literature. Yet, we wanted to raise this question again because the misconception of a first-order phase transition between the inhomogeneous and homogeneous NS matter (with electrons) is rather widespread among researchers. It is important to keep in mind, however, that, while there is no thermodynamic instability, the inhomogeneous stellar matter does transform into homogeneous one by dissolution or disintegration of clusters. The physical mechanism of disintegration of clusters is mentioned, e.g., in Ref. [38] in the context of accreted crusts. The mechanism of dissolution is discussed in Ref. [47].

## IV. CONCLUSIONS

An extended NSE model [8] was employed here to compute the properties of finite temperature inhomogeneous matter pertaining to the crusts of neo-NSs.

The three main messages of this Letter are: 1. A possible presence of an almost pure  $^{14}\text{He}$  layer in the innermost shells of the NSs crusts was pointed out. In addition to challenging nuclear pasta phases, this layer will affect the transport properties of the crust as well as the process of crust crystallization. To the best of our knowledge, this was not discussed before. 2. The problem of the stability with respect to diffusion of ions (buoyancy) in the inner crusts of neo-NSs was introduced and briefly examined. While the crusts presented in this Letter are stable, some of the crusts previously put forward in the literature are not. As far as we know, this question was not previously considered. 3. Finally, we demonstrated that in NS matter, the transition from inhomogeneous to homogeneous matter does not correspond to a first-order phase transition. As this is a common misconception, it is important to emphasize this aspect again, even if it was known before.

## ACKNOWLEDGMENTS

The authors acknowledge support from a grant from the Ministry of Research, Innovation and Digitization, CNCS/CCCDI-UEFISCDI, Project No. PN-IV-P1-PCE-2023-0324; partial support from Project No. PN 23 21 01 02 is also acknowledged.

M.V.B. and A.R.R. contributed equally to this work.

- 
- [1] M. V. Beznogov, D. Page, and E. Ramirez-Ruiz, Thermal Evolution of Neo-neutron Stars. I. Envelopes, Eddington Luminosity Phase, and Implications for GW170817, *Astrophys. J.* **888**, 97 (2020).
  - [2] A. F. Fantina, S. De Ridder, N. Chamel, and F. Gulminelli, Crystallization of the outer crust of a non-accreting neutron star, *Astron. Astrophys.* **633**, A149 (2020).
  - [3] T. Carreau, F. Gulminelli, N. Chamel, A. F. Fantina, and J. M. Pearson, Crystallization of the inner crust of a neutron star and the influence of shell effects, *Astron. Astrophys.* **635**, A84 (2020).
  - [4] N. Chamel and P. Haensel, Physics of Neutron Star Crusts, *Liv. Rev. Relat.* **11**, 10 (2008).
  - [5] A. Y. Potekhin and G. Chabrier, Crust structure and thermal evolution of neutron stars in soft X-ray transients, *Astron. Astrophys.* **645**, A102 (2021).
  - [6] P. Haensel, A. Y. Potekhin, and D. G. Yakovlev, *Neutron Stars. I. Equation of State and Structure*, Astrophysics and Space Science Library, Vol. 326 (Springer, New York, 2007).
  - [7] L. Suleiman, J. L. Zdunik, P. Haensel, and M. Fortin, Partially accreted crusts of neutron stars, *Astron. Astrophys.* **662**, A63 (2022).
  - [8] A. R. Raduta and M. V. Beznogov, New ab initio constrained extended Skyrme equations of state for simulations of neutron stars, supernovae and binary mergers: I. Subsaturating density domain, in preparation (2025).
  - [9] M. Hempel and J. Schaffner-Bielich, A statistical model for a complete supernova equation of state, *Nucl. Phys. A* **837**, 210 (2010).
  - [10] M. Wiescher and T. Rauscher, Nuclear reactions, in *Astrophysics with Radioactive Isotopes*, edited by R. Diehl, D. H. Hartmann, and N. Prantzos (Springer International Publishing, Cham, 2018) pp. 523–554.
  - [11] J. M. Lattimer, C. J. Pethick, D. G. Ravenhall, and D. Q. Lamb, Physical properties of hot, dense matter: The general case, *Nucl. Phys. A* **432**, 646 (1985).
  - [12] M. Wang, W. J. Huang, F. G. Kondev, G. Audi, and S. Naimi, The AME 2020 atomic mass evaluation (II). Tables, graphs and references, *Chin. Phys. C* **45**, 030003 (2021).
  - [13] J. Duflo and A. P. Zuker, Microscopic mass formulae, *Phys. Rev. C* **52**, R23 (1995).
  - [14] D. Bucurescu and T. von Egidy, Correlations between the nuclear level density parameters, *Phys. Rev. C* **72**, 067304 (2005).
  - [15] T. von Egidy and D. Bucurescu, Systematics of nuclear level density parameters, *Phys. Rev. C* **72**, 044311 (2005), [Erratum: *Phys. Rev. C* **73**, 049901 (2006)].
  - [16] J. W. Negele and D. Vautherin, Density-Matrix Expansion for an Effective Nuclear Hamiltonian, *Phys. Rev. C* **5**, 1472 (1972).
  - [17] D. Vautherin, Many-body methods at finite temperature, in *Advances in Nuclear Physics*, edited by J. W. Negele and E. Vogt

- (Springer US, Boston, MA, 1996) pp. 123–172.
- [18] S. Goriely, N. Chamel, and J. M. Pearson, Further explorations of Skyrme-Hartree-Fock-Bogoliubov mass formulas. 13. The 2012 atomic mass evaluation and the symmetry coefficient, *Phys. Rev. C* **88**, 024308 (2013).
  - [19] M. G. Alford and S. P. Harris,  $\beta$  equilibrium in neutron-star mergers, *Phys. Rev. C* **98**, 065806 (2018).
  - [20] J. M. Pearson, N. Chamel, A. Y. Potekhin, A. F. Fantina, C. Ducoin, A. K. Dutta, and S. Goriely, Unified equations of state for cold non-accreting neutron stars with Brussels–Montreal functionals – I. Role of symmetry energy, *Mon. Not. Roy. Astron. Soc.* **481**, 2994 (2018), [Erratum: *Mon. Not. Roy. Astron. Soc.* **486**, 768 (2019)].
  - [21] A. Schmitt and P. Shternin, Reaction Rates and Transport in Neutron Stars, in *Astrophysics and Space Science Library*, Astrophysics and Space Science Library, Vol. 457, edited by L. Rezzolla, P. Pizzochero, D. I. Jones, N. Rea, and I. Vidaña (2018) p. 455, arXiv:1711.06520 [astro-ph.HE].
  - [22] Notice, however, that our results refer to non-accreted crusts, while low mass X-ray binaries have partially or fully accreted crusts.
  - [23] A. Y. Potekhin, A. I. Chugunov, and G. Chabrier, Thermal evolution and quiescent emission of transiently accreting neutron stars, *Astron. Astrophys.* **629**, A88 (2019).
  - [24] J. A. Pons, D. Viganò, and N. Rea, A highly resistive layer within the crust of X-ray pulsars limits their spin periods, *Nat. Phys.* **9**, 431 (2013).
  - [25] S. Typel, G. Ropke, T. Klahn, D. Blaschke, and H. H. Wolter, Composition and thermodynamics of nuclear matter with light clusters, *Phys. Rev. C* **81**, 015803 (2010).
  - [26] P. Papakonstantinou, J. Margueron, F. Gulminelli, and A. R. Raduta, Densities and energies of nuclei in dilute matter at zero temperature, *Phys. Rev. C* **88**, 045805 (2013).
  - [27] O. Ivanytskyi, M. Ángeles Pérez-García, and C. Albertus, Tetra-neutron condensation in neutron rich matter, *Eur. Phys. J. A* **55**, 184 (2019).
  - [28] H. Pais, C. Albertus, M. Á. Pérez-García, and C. Providência, Influence of the tetra-neutron on the EoS under core-collapse supernova and heavy-ion collision conditions, *Astron. Astrophys.* **679**, A113 (2023).
  - [29] P. Chang, L. Bildsten, and P. Arras, Diffusive Nuclear Burning of Helium on Neutron Stars, *Astrophys. J.* **723**, 719 (2010).
  - [30] M. V. Beznogov and D. G. Yakovlev, Diffusion and Coulomb Separation of Ions in Dense Matter, *Phys. Rev. Lett* **111**, 161101 (2013).
  - [31] M. V. Beznogov, A. Y. Potekhin, and D. G. Yakovlev, Diffusive heat blanketing envelopes of neutron stars, *Mon. Not. Roy. Astron. Soc.* **459**, 1569 (2016).
  - [32] One has to keep in mind that the temperature distribution inside a neo-NS is strongly non-uniform.
  - [33] F. Grill, H. Pais, C. Providência, I. Vidaña, and S. S. Avancini, Equation of state and thickness of the inner crust of neutron stars, *Phys. Rev. C* **90**, 045803 (2014).
  - [34] J. W. Negele and D. Vautherin, Neutron star matter at sub-nuclear densities, *Nucl. Phys. A* **207**, 298 (1973).
  - [35] X. Viñas, C. Gonzalez-Boquera, M. Centelles, C. Mondal, and L. M. Robledo, Unified Equation of State for Neutron Stars Based on the Gogny Interaction, *Symm.* **13**, 1613 (2021).
  - [36] L. Scurto, H. Pais, and F. Gulminelli, General predictions of neutron star properties using unified relativistic mean-field equations of state, *Phys. Rev. D* **109**, 103015 (2024).
  - [37] A. I. Chugunov and N. N. Shchepochin, Crucial role of neutron diffusion in the crust of accreting neutron stars, *Mon. Not. Roy. Astron. Soc.* **495**, L32 (2020).
  - [38] M. E. Gusakov and A. I. Chugunov, Thermodynamically Consistent Equation of State for an Accreted Neutron Star Crust, *Phys. Rev. Lett.* **124**, 191101 (2020).
  - [39] H. Müller and B. D. Serot, Phase transitions in warm, asymmetric nuclear matter, *Phys. Rev. C* **52**, 2072 (1995).
  - [40] C. Ducoin, P. Chomaz, and F. Gulminelli, Role of isospin in the nuclear liquid–gas phase transition, *Nucl. Phys. A* **771**, 68 (2006).
  - [41] I. Vidana and A. Polls, Spinodal instabilities of asymmetric nuclear matter within the Brueckner-Hartree-Fock approach, *Phys. Lett. B* **666**, 232 (2008).
  - [42] A. Carbone, A. Polls, and A. Rios, Microscopic Predictions of the Nuclear Matter Liquid-Gas Phase Transition, *Phys. Rev. C* **98**, 025804 (2018).
  - [43] C. Ducoin, P. Chomaz, and F. Gulminelli, Isospin-dependent clusterization of Neutron-Star Matter, *Nucl. Phys. A* **789**, 403 (2007).
  - [44] To be more precise, for the inhomogeneous matter the electron contribution was subtracted, but the Coulomb contribution remained as if the electrons were present.
  - [45] A. R. Raduta and F. Gulminelli, Thermodynamics of clusterized matter, *Phys. Rev. C* **80**, 024606 (2009).
  - [46] A. R. Raduta and F. Gulminelli, Statistical description of complex nuclear phases in supernovae and proto-neutron stars, *Phys. Rev. C* **82**, 065801 (2010).
  - [47] H. Pais and S. Typel, Comparison of equation of state models with different cluster dissolution mechanisms, in *Nuclear Particle Correlations and Cluster Physics*, edited by S. Wolf-Udo (WORLD SCIENTIFIC, 2017) pp. 95–132, arXiv:1612.07022 [nucl-th].